Ligation of protease-activated receptor 1 enhances $\alpha_v\beta_6$ integrin–dependent TGF-β activation and promotes acute lung injury

R. Gisli Jenkins,[1,2] Xiao Su,[3] George Su,[1] Christopher J. Scotton,[2] Eric Camerer,[3] Geoffrey J. Laurent,[2] George E. Davis,[4] Rachel C. Chambers,[2] Michael A. Matthay,[3] and Dean Sheppard[1]

[1]Lung Biology Center, UCSF, San Francisco, California, USA. [2]Centre for Respiratory Research, University College London, London, United Kingdom. [3]Cardiovascular Research Institute, UCSF, San Francisco, California, USA. [4]Department of Pathology and Laboratory Medicine, Texas A&M University System Health Science Center, College Station, Texas, USA.

Activation of latent TGF-β by the $\alpha_v\beta_6$ integrin is a critical step in the development of acute lung injury. However, the mechanism by which $\alpha_v\beta_6$-mediated TGF-β activation is regulated has not been identified. We show that thrombin, and other agonists of protease-activated receptor 1 (PAR1), activate TGF-β in an $\alpha_v\beta_6$ integrin–specific manner. This effect is PAR1 specific and is mediated by RhoA and Rho kinase. Intratracheal instillation of the PAR1-specific peptide TFLLRN increases lung edema during high-tidal-volume ventilation, and this effect is completely inhibited by a blocking antibody against the $\alpha_v\beta_6$ integrin. Instillation of TFLLRN during high-tidal-volume ventilation is associated with increased pulmonary TGF-β activation; however, this is not observed in *Itgb6*$^{-/-}$ mice. Furthermore, *Itgb6*$^{-/-}$ mice are also protected from ventilator-induced lung edema. We also demonstrate that pulmonary edema and TGF-β activity are similarly reduced in *Par1*$^{-/-}$ mice following bleomycin-induced lung injury. These results suggest that PAR1-mediated enhancement of $\alpha_v\beta_6$-dependent TGF-β activation could be one mechanism by which activation of the coagulation cascade contributes to the development of acute lung injury, and they identify PAR1 and the $\alpha_v\beta_6$ integrin as potential therapeutic targets in this condition.

Introduction

Integrins are heterodimeric transmembrane proteins involved in cell-cell and cell-matrix interactions. There are 24 known human integrins, including 8 that generally recognize ligands that contain an arginine-glycine-aspartate (RGD) sequence. Two of these integrins ($\alpha_v\beta_6$ and $\alpha_v\beta_8$) bind the RGD sequence in the latency-associated peptide (LAP) of TGF-β1 and -β3 and activate latent TGF-β (1, 2). TGF-β is a pleiotropic cytokine that has crucial homeostatic, immunologic, and developmental functions. Activation of the latent TGF-β complex is a critical step in regulating the biological availability of this molecule and its subsequent actions. Although there are numerous mechanisms by which latent TGF-β may be activated in vitro (2–7), activation by the $\alpha_v\beta_6$ integrin has been shown to be important in models of a number of disease processes, including pulmonary and renal fibrosis, pulmonary emphysema, and acute lung injury (1, 8–10).

It is not currently known how the $\alpha_v\beta_6$ integrin activates latent TGF-β. It is likely that the $\alpha_v\beta_6$ integrin needs to be activated itself, because tissue-specific overexpression of the β_6 integrin subunit, in the absence of injury, does not lead to TGF-β activation or tissue fibrosis (11, 12). We have previously shown that $\alpha_v\beta_6$ integrin–mediated TGF-β activity is dependent on cytoskeletal integrity. Inhibition of actin assembly by cytochalasin, and β_6 subunit cytoplasmic truncation mutants that prevent integrin interaction with the actin cytoskeleton, each abolish TGF-β activation by $\alpha_v\beta_6$ (1). Activation of TGF-β by $\alpha_v\beta_6$ probably requires more than simply binding to LAP, as we have identified cytoplasmic mutants that bind LAP but do not activate TGF-β. Furthermore the $\alpha_v\beta_1$ (13) and $\alpha_8\beta_1$ integrins (14) are both able to bind LAP but do not activate TGF-β.

Thrombin, a serine protease that is involved in hemostasis, is generated early during acute lung injury and is thought to contribute to increased lung permeability (15, 16). Furthermore, thrombin is a potent activator of the platelet integrin $\alpha_{IIb}\beta_3$ via its actions on the protease-activated receptors (PARs). In mice the cellular effects of thrombin are mediated through PAR1 and PAR4, with both receptors mediating platelet responses and PAR1 being the predominant PAR in lung fibroblasts (17, 18). PAR1 is also present in lung epithelium and is upregulated in response to lung injury (19). PAR1 is a 7-transmembrane-domain G protein–coupled receptor that couples to heterotrimeric G proteins of the Gαi, Gαq, and Gα12/13 families.

The purpose of the present study was to define a mechanism through which the $\alpha_v\beta_6$ integrin may be activated following injury. We demonstrate that 3 different ligands for PAR1, including thrombin, are able to activate TGF-β in an $\alpha_v\beta_6$-dependent manner, and that PAR1 signals to $\alpha_v\beta_6$ through RhoA and Rho kinase. Furthermore, we show that this pathway is relevant to the development of pulmonary edema in 2 different in vivo models.

Results

Characterization of Immortomouse lung epithelial cells. To take advantage of genetic approaches to study $\alpha_v\beta_6$-dependent TGF-β activa-

Nonstandard abbreviations used: ELW, excess lung water; EVPE, extravascular plasma equivalents; IMLE, Immortomouse lung epithelial (cell); LAP, latency-associated peptide; LTBP-1, latent TGF-β–binding protein-1; PAR, protease-activated receptor; TML, transformed mink lung.

Conflict of interest: The authors have declared that no conflict of interest exists.

Citation for this article: *J. Clin. Invest.* **116**:1606–1614 (2006). doi:10.1172/JCI27183.

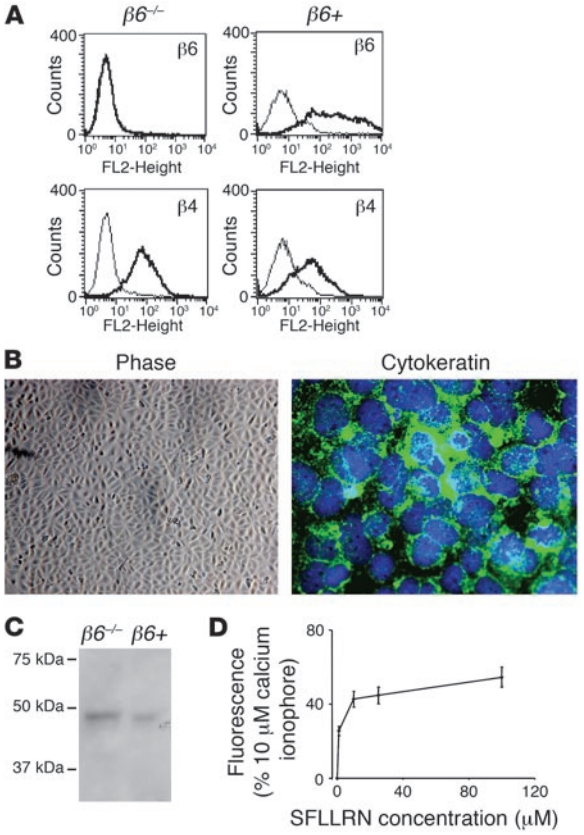

Figure 1
IMLE cells express epithelial cell markers and functional PAR1. (**A**) β_6 and β_4 integrin subunit cell surface expression on *Itgb6*$^{-/-}$ Immortomouse cells was analyzed before ($\beta6^{-/-}$) and after ($\beta6$+) infection with a retroviral vector encoding human WT β_6. (**B**) Epithelial cell morphology was observed by phase-contrast light microscopy (×100), and expression of the epithelial marker cytokeratin was determined by immunofluorescence using a FITC-labeled primary antibody (×600). (**C**) Presence of the PAR1 receptor in IMLE cells was analyzed by Western blotting of cell lysates using a specific anti-PAR1 antibody. (**D**) To determine whether the PAR1 in these cells was functional, cell suspensions were treated with increasing doses of the PAR1-activating peptide SFLLRN, and increasing calcium mobilization was determined as a percentage of the positive control, 10 μM calcium ionophore.

tion, we harvested lung epithelial cells from *Itgb6*$^{-/-}$ mice that had been crossed to a line (Immortomouse) expressing a temperature-sensitive large T antigen transgene. To determine whether the cells harvested from the lung of the *Itgb6*$^{-/-}$ Immortomouse were epithelial in origin, cells were assessed by flow cytometry (Figure 1A) and phase-contrast light microscopy (Figure 1B). Before retroviral infection with the β_6 integrin subunit, lung epithelial cells expressed no β_6 but high levels of the β_4 subunit. After retroviral infection, the β_4 integrin was still expressed along with high levels of β_6 (Figure 1A). The epithelial derivation of these cells was confirmed by the presence of the epithelial cell marker cytokeratin (Figure 1B). To determine whether PAR1 was present, Western analysis was performed on epithelial cell lysates (Figure 1C). A band was seen at the expected molecular weight in lysates from both β_6-positive and β_6-negative cells, confirming the presence of the receptor. To determine whether this receptor was functional, calcium mobilization studies were performed (Figure 1D). The PAR1-activating peptide SFLLRN induced a dose-dependent increase in fluorescence intensity, demonstrating that these receptors function normally in Immortomouse lung epithelial (IMLE) cells.

PAR1-activating peptides and thrombin enhance $\alpha_v\beta_6$-mediated TGF-β activation. The PAR1-activating peptide SFLLRN was used to stimulate the IMLE cells in coculture with transformed mink lung (TML) reporter cells containing the TGF-β–responsive plasminogen activator inhibitor-1 promoter driving luciferase expression. SFLLRN induced a dose-dependent increase in luciferase activity in cells expressing $\alpha_v\beta_6$ that was completely abolished by $\alpha_v\beta_6$ blocking antibody (Figure 2A). SFLLRN had no effect on *Itgb6*$^{-/-}$ IMLE cells, and no inhibitory effect of the $\alpha_v\beta_6$ blocking antibody was observed (Figure 2A). To determine the proportion of PAR1-induced TGF-β activity that was mediated by $\alpha_v\beta_6$, a pan–TGF-β blocking antibody was used. The effects of blocking $\alpha_v\beta_6$ or TGF-β were essentially the same, demonstrating that there was no $\alpha_v\beta_6$-independent TGF-β activation by these cells (Figure 2B). Because IMLE cells are an immortalized cell line that might not be identical to primary lung epithelial cells, we performed the same experiments in primary human bronchial epithelial cells. SFLLRN also induced TGF-β activity in these cells, and all TGF-β activity was inhibited by the $\alpha_v\beta_6$ blocking antibody (Figure 2B).

To determine the time course of PAR1-induced $\alpha_v\beta_6$-mediated TGF-β activity, SMAD2 phosphorylation in IMLE monolayers was assessed in the absence of TML cells. Thrombin and the PAR1-activating peptide SFLLRN were both used to stimulate IMLE cells, and both agonists caused a time-dependent increase in Smad2 phosphorylation (Figure 3, A and B). A slight increase in Smad2 phosphorylation was observed after 15 minutes, and the signal increased over time, being maximal at 4 hours. Thrombin- and PAR1 agonist–induced Smad2 phosphorylation was completely blocked by anti-$\alpha_v\beta_6$ blocking antibody, confirming that PAR1-mediated TGF-β activation in pulmonary epithelial cells is entirely mediated by $\alpha_v\beta_6$.

The protracted time course of Smad2 phosphorylation in response to PAR1 stimulation suggested the possibility that new protein synthesis might be required. To test this hypothesis, Smad2 phosphorylation was assessed in response to SFLLRN in the presence of the protein synthesis inhibitor cycloheximide (Figure 3C). Cycloheximide did not inhibit PAR1-induced Smad2 phosphorylation, despite inhibiting total Smad2 levels, indicating that PAR1-induced Smad2 phosphorylation does not require new protein synthesis.

PAR1-activating peptide–induced $\alpha_v\beta_6$-mediated TGF-β activation is mediated via PAR1. To confirm that the PAR1-activating peptide SFLLRN was acting specifically via PAR1, we assessed $\alpha_v\beta_6$-mediated TGF-β activation in fibroblasts that had been stably transfected with β_6, to enable subsequent assessment in fibroblasts from *Par1*$^{-/-}$ mice. In WT mouse embryonic fibroblasts, the PAR1-activating peptides SFLLRN and TFLLRN induced a dose-dependent increase in $\alpha_v\beta_6$-dependent TGF-β activity, but a scrambled peptide had no effect (Figure 4A). SFLLRN is known to also activate PAR2 in some circumstances (20, 21), but there was no effect of the PAR2 agonist SLIGRL (data not shown). Having demonstrated that PAR1 agonists can activate TGF-β via $\alpha_v\beta_6$ in fibroblasts, we stably transfected *Par1*$^{-/-}$ lung fibroblasts, as well as fibroblasts that had been reconstituted with WT PAR1, with the β_6 subunit. Both *Par1*$^{-/-}$ and WT reconstituted fibroblasts expressed similar levels of $\alpha_v\beta_6$ after transfection (Figure 4B); however, only the WT reconsti-

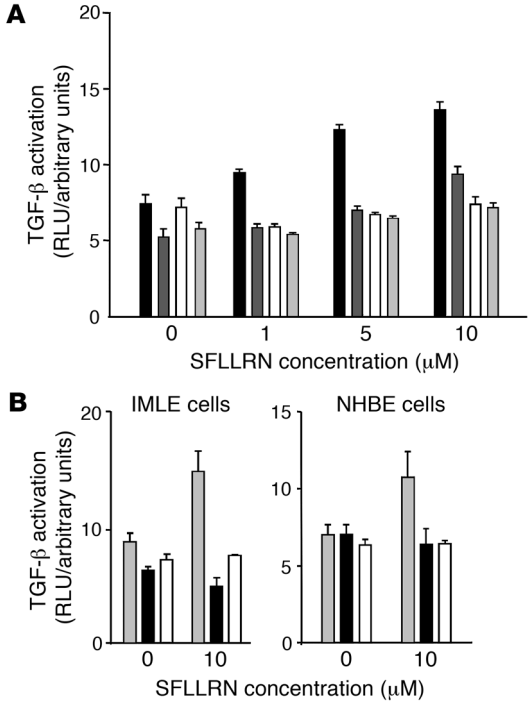

Figure 2
Stimulation of lung epithelial cells with a PAR1 agonist leads to $\alpha_v\beta_6$-dependent TGF-β activation. (**A**) IMLE cells were cocultured with TML cells and stimulated with increasing doses of SFLLRN, and luciferase activity from the TGF-β–responsive plasminogen activator inhibitor-1 promoter was measured. IMLE cells expressing human WT β_6 (black bars) were compared with IMLE cells that had no cell surface β_6 (white bars), and both were also stimulated with increasing doses of SFLLRN in the presence of $\alpha_v\beta_6$ blocking antibody (IMLE β_6-positive, dark gray bars; IMLE β_6-negative, light gray bars). (**B**) To determine the proportion of TGF-β expression that was mediated by $\alpha_v\beta_6$ in epithelial cell cultures, IMLE cells and normal human bronchial epithelial (NHBE) cells were stimulated with 10 μM of SFLLRN (gray bars), in the absence or presence of an $\alpha_v\beta_6$ blocking antibody (black bars) or a pan–TGF-β blocking antibody (white bars), in coculture with TML cells, and luciferase activity was measured. All experiments were performed in triplicate, and the mean + SEM is shown. Results are a representative example of at least 2 identical independent experiments.

tuted fibroblasts activated TGF-β in an $\alpha_v\beta_6$-dependent manner in response to the PAR1 agonist SFLLRN (Figure 4C).

PAR1 signals to the $\alpha_v\beta_6$ integrin via RhoA and Rho kinase. We have previously shown that the actin cytoskeleton is critical in $\alpha_v\beta_6$-mediated TGF-β activation (1). We therefore hypothesized that the signal would be mediated via the small GTPase RhoA, which is known to be activated by PAR1 and to be critical for active reorganization of cellular actin. To investigate the role of RhoA, we infected β_6-transfected fibroblasts with adenoviruses expressing either constitutively active or dominant-negative forms of RhoA, together with GFP to allow subsequent sorting for infected cells. Constitutively active Rho induced a large increase in $\alpha_v\beta_6$-mediated TGF-β activity that was not further enhanced by stimulation with a PAR1 agonist, whereas cells infected with GFP alone had the characteristic increase in TGF-β activity in response to PAR1 stimulation (Figure 5A). Dominant-negative RhoA did not affect baseline $\alpha_v\beta_6$-mediated TGF-β activity but inhibited the increase of $\alpha_v\beta_6$-mediated TGF-β activation in response to SFLLRN (Figure 5A). There was no difference in baseline or induced TGF-β activity following transfection of fibroblasts with GFP compared with untransfected cells (data not shown). To confirm that RhoA was acting downstream of the PAR1 receptor in mediating signals to $\alpha_v\beta_6$, *Par1*$^{-/-}$ fibroblasts expressing $\alpha_v\beta_6$ were transiently infected with the adenoviral constructs as described. As with WT fibroblasts, the constitutively active RhoA construct was able to activate TGF-β via $\alpha_v\beta_6$ (Figure 5A), confirming that RhoA is downstream of the PAR1 receptor in this pathway.

Because RhoA is known to activate Rho kinase, we assessed the effect of the Rho kinase inhibitor Y-27632 on PAR1-induced

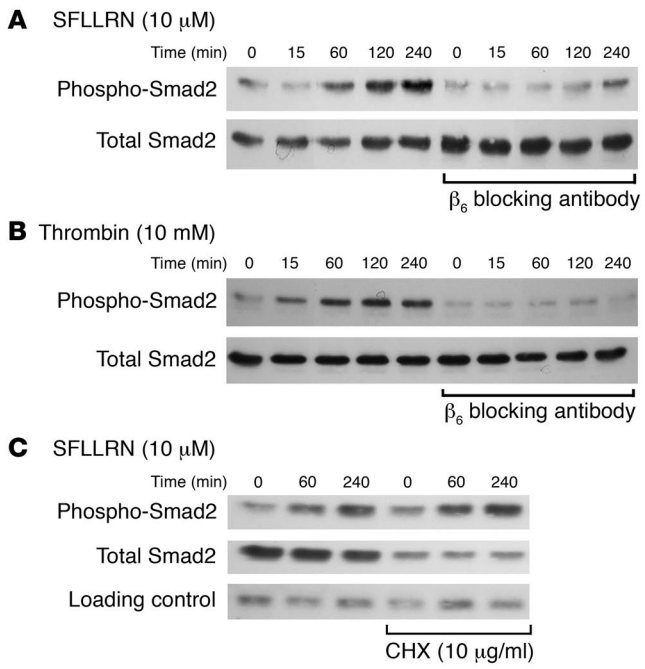

Figure 3
PAR1 agonists lead to a time-dependent increase in Smad2 phosphorylation that is $\alpha_v\beta_6$ integrin dependent, but independent of new protein synthesis. (**A** and **B**) The time course of Smad2 phosphorylation in response to 10 μM PAR1-activating peptide SFLLRN (**A**) and 10 nM thrombin (**B**), in the presence or absence of an $\alpha_v\beta_6$ blocking antibody, was assessed by immunoblotting. Total Smad2 levels over time and in response to the $\alpha_v\beta_6$ blocking antibody were assessed as control. (**C**) Immunoblot showing the effect of the protein synthesis inhibitor cycloheximide (CHX) on SFLLRN-induced Smad2 phosphorylation. The effectiveness of cycloheximide as a protein synthesis inhibitor was determined by immunoblotting for total Smad2, and immunoblotting for MyD88 was used as a loading control.

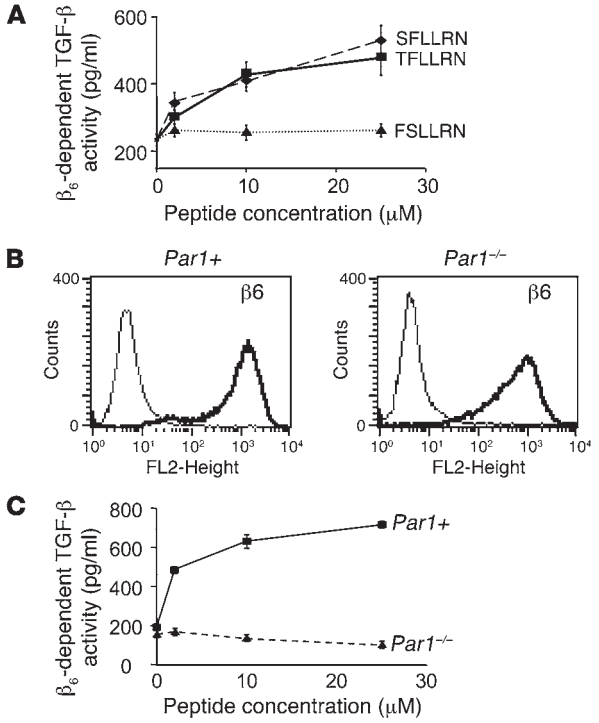

Figure 4
PAR1 peptide–induced $\alpha_v\beta_6$-dependent TGF-β activity is PAR1 receptor specific. (**A**) $\alpha_v\beta_6$-dependent TGF-β activity following stimulation of mouse embryonic fibroblast cells, stably transfected with human WT β_6, with increasing doses of the PAR1-activating peptides TFLLRN and SFLLRN or the scrambled peptide control (FSLLRN), which has no known PAR1-activating effect. $\alpha_v\beta_6$-dependent TGF-β activity was calculated from coculture bioassays with TML cells, by comparison of the difference in luciferase activity in the absence and presence of $\alpha_v\beta_6$ blocking antibody with values obtained from a standard curve performed in coculture experiments with increasing concentrations of recombinant TGF-β. (**B**) After infection with a retroviral vector expressing WT human β_6, $\alpha_v\beta_6$ expression in lung fibroblasts from *Par1*$^{-/-}$ mice that were either null (*Par1*$^{-/-}$) or reconstituted with WT PAR1 (*Par1*+) was assessed by flow cytometry. (**C**) $\alpha_v\beta_6$-expressing *Par1*$^{-/-}$ and *Par1*+ fibroblasts were stimulated with increasing doses of SFLLRN, and $\alpha_v\beta_6$-dependent TGF-β activity was measured by coculture bioassay.

$\alpha_v\beta_6$-mediated TGF-β activation (Figure 5, B and C). In both IMLE cells and murine fibroblasts, Y-27632 caused dose-dependent inhibition of $\alpha_v\beta_6$-mediated TGF-β activity induced by 10 μM SFLLRN, with an IC_{50} of approximately 0.8 μM. High concentrations of the Rho kinase inhibitor had a small effect on recombinant TGF-β–induced TGF-β activity, as measured by the TML cell reporter bioassay. Therefore, we assessed the effect of Y-27632 on SFLLRN- and recombinant TGF-β–induced Smad2 phosphorylation (Figure 5C). SFLLRN-induced Smad2 phosphorylation was inhibited by either $\alpha_v\beta_6$ blocking antibody or Y-27632, whereas TGF-β–induced Smad2 phosphorylation was not inhibited by either the blocking antibody or Y-27632, confirming that PAR1-induced $\alpha_v\beta_6$-mediated TGF-β activation requires Rho kinase activity.

PAR1 stimulation exacerbates ventilator-associated pulmonary edema, and this effect is mediated by the $\alpha_v\beta_6$ integrin. To determine whether PAR1-mediated enhancement of $\alpha_v\beta_6$-dependent TGF-β activation would be relevant in vivo, we examined the effects of a PAR1-activating peptide in a model of noncardiogenic pulmonary edema induced by high-tidal-volume ventilation. In preliminary studies we determined that in untreated mice, 2 hours of high-tidal-volume ventilation was insufficient to increase either excess lung water (ELW; Figure 6A) or the extravasation of ^{125}I-labeled albumin into the lungs (extravascular plasma equivalents [EVPE]; Figure 6B). Under the same conditions, intratracheal instillation of PAR1 agonist (TFLLRN) significantly increased both ELW (Figure 6A) and EVPE (Figure 6B), compared with vehicle and its control peptide (FTLLRN). Systemic administration of an $\alpha_v\beta_6$ blocking

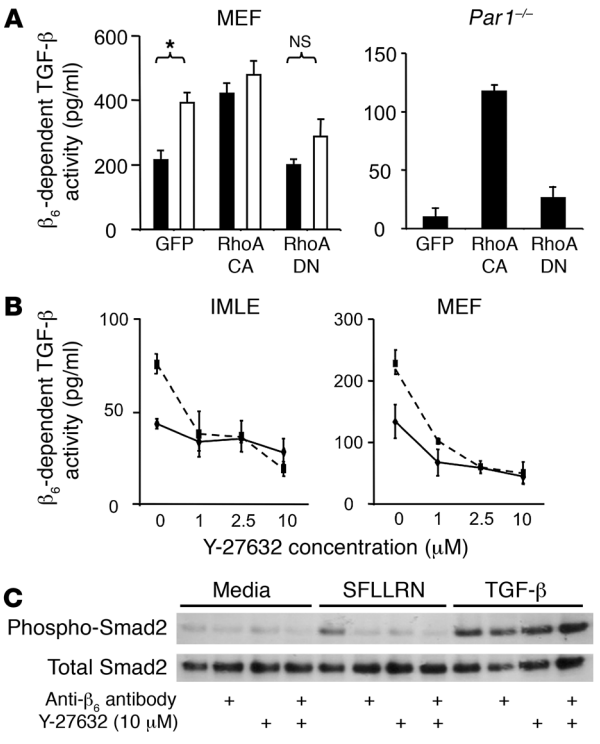

Figure 5
PAR1 signals via RhoA and Rho kinase to induce $\alpha_v\beta_6$-mediated TGF-β activation. (**A**) WT mouse embryonic fibroblasts expressing $\alpha_v\beta_6$ (MEFβ6) were adenovirally infected with GFP, constitutively active (CA) RhoA, or dominant-negative (DN) RhoA. After infection and cell sorting, cells were stimulated (white bars) or were not stimulated (black bars) with 10 μM SFLLRN, and β_6-dependent TGF-β activity was calculated from coculture bioassays with TML cells. Unstimulated *Par1*$^{-/-}$ cells expressing $\alpha_v\beta_6$ were also infected with an adenovirus encoding a constitutively active RhoA, dominant-negative RhoA, or GFP control and studied in coculture bioassays, as above. (**B**) IMLE cells and mouse embryonic fibroblasts, both expressing the β_6 integrin, were stimulated with 10 μM SFLLRN (dashed lines) in the presence of increasing doses of the Rho kinase inhibitor Y-27632, and $\alpha_v\beta_6$-mediated TGF-β activity was compared with that of unstimulated IMLE cells (solid lines). (**C**) MEFβ6 cells were stimulated with 10 μM SFLLRN or 500 pg/ml TGF-β for 4 hours in the presence or absence of the Rho kinase inhibitor Y-27632 and an $\alpha_v\beta_6$ blocking antibody, and compared with unstimulated cells. Cell lysates were analyzed by Western blotting for phospho-Smad2 or total Smad2. All results are representative of at least 3 independent experiments. *$P < 0.005$.

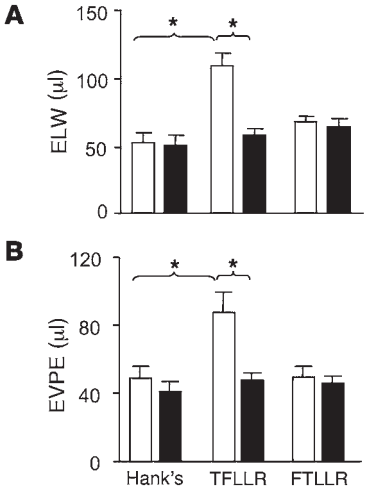

Figure 6
PAR1-induced pulmonary edema is mediated by the $\alpha_v\beta_6$ integrin. (**A**) Mice were pretreated with control nonblocking antibody (white bars) or $\alpha_v\beta_6$ blocking antibody (black bars) before ventilation at 24 ml/kg and intratracheal instillation with PAR1-specific peptide (TFLLRN), vehicle (HBSS), or peptide control (FTLLRN). ELW was measured as the wet-to-dry weight ratio of excised lungs. (**B**) Mice were pretreated with control nonblocking antibody (white bars) or $\alpha_v\beta_6$ blocking antibody (black bars) before ventilation at 24 ml/kg and intratracheal instillation of peptide and controls. Lung extravascular plasma equivalents were calculated based on the extravasation of ^{125}I-labeled albumin into the lungs. Hank's, $n = 8$; TFLLRN, $n = 10$; and FTLLRN, $n = 11$. Values are presented as mean + SEM. *$P < 0.01$.

antibody completely prevented the increases in ELW and EVPE induced by the PAR1 agonist peptide but had no effect on either variable in mice treated with vehicle or with the control peptide.

Itgb6$^{-/-}$ mice are protected from PAR1-mediated ventilator-associated pulmonary edema, and this is associated with reduced TGF-β activity in the lung. To confirm the role of $\alpha_v\beta_6$-mediated TGF-β activation in the development of PAR1-mediated ventilator-associated pulmonary edema, we examined the effect of PAR1-activating peptides in high-tidal-volume ventilation in *Itgb6$^{-/-}$* mice (Figure 7). Instillation of TFLLRN followed by 2 hours of high-tidal-volume ventilation caused a significant increase in ELW in WT mice, whereas the *Itgb6$^{-/-}$* mice showed levels of protection similar to that observed following administration of the $\alpha_v\beta_6$ blocking antibody (Figure 7A). A similar effect was also measured by EVPE (data not shown). To confirm that PAR1 could enhance TGF-β activity during high-tidal-volume ventilation, nuclear localized phosphorylated Smad2 levels were measured by immunohistochemistry. In WT mice instilled with Hank's solution, there was very little baseline TGF-β activity, and this was markedly increased following instillation of TFLLRN (Figure 7, B and C). However, there was no significant increase in Smad2 phosphorylation in *Itgb6$^{-/-}$* mice treated with TFLLRN (Figure 7, B and C).

Par1$^{-/-}$ mice are protected from bleomycin-induced permeability changes and in vivo TGF-β activation. Having demonstrated that stimulation of PAR1 can lead to $\alpha_v\beta_6$-mediated TGF-β activity and increased lung edema in vivo, we sought to determine whether *Par1$^{-/-}$* mice would be protected from permeability changes in another model of acute lung injury. We used the bleomycin model because the effects of bleomycin have previously been shown to be mediated by the $\alpha_v\beta_6$ integrin (9). As expected, bleomycin significantly increased lung permeability in WT mice (Figure 8A), but this effect was significantly reduced in *Par1$^{-/-}$* mice. To determine whether this protection was associated with a reduction in TGF-β activity in the lung, we assessed the presence of phosphorylated Smad2. In WT mice, bleomycin treatment significantly increased nuclear phosphorylated Smad2 immunoreactivity, but this effect was significantly reduced in *Par1$^{-/-}$* mice (Figure 8, B and C).

Discussion

Previous work from our laboratory strongly suggested that binding of the $\alpha_v\beta_6$ integrin to the LAP of TGF-β was necessary but not sufficient to activate latent complexes of TGF-β, implying that this process could be regulated. However, until now the

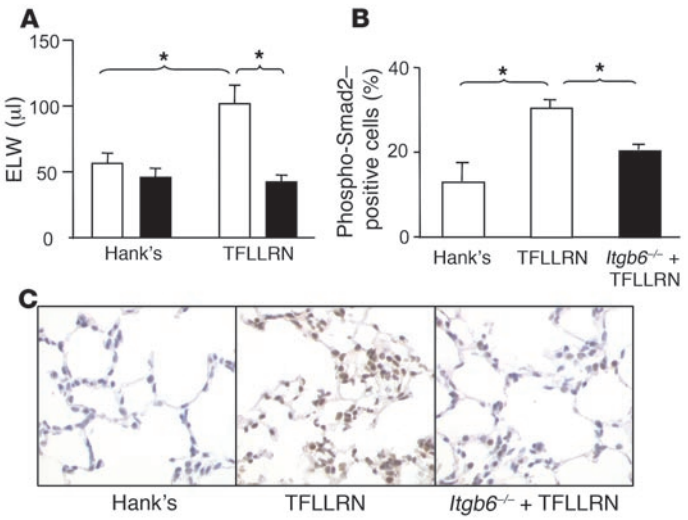

Figure 7
Itgb6$^{-/-}$ mice instilled with TFLLRN and ventilated at high tidal volume are protected from lung edema and have reduced TGF-β activity in the lung compared with WT mice. (**A**) WT mice (white bars) and *Itgb6$^{-/-}$* mice (black bars) were ventilated and instilled with peptide and control, and lung edema was measured as described previously. WT, $n = 6$; and *Itgb6$^{-/-}$*, $n = 5$. (**B**) Quantification of nuclear localized phospho-Smad2 immunostaining in WT mice instilled with Hank's or PAR1-activating peptide or *Itgb6$^{-/-}$* mice instilled with PAR1-activating peptide (black bar). WT mice, Hank's, $n = 3$; WT mice, TFLLRN, $n = 4$; *Itgb6$^{-/-}$* mice, $n = 3$; and *Par1$^{-/-}$* mice, saline, $n = 3$. (**C**) Representative histological sections showing nuclear localized phospho-Smad2 immunostaining in the lung of WT or *Itgb6$^{-/-}$* mice. Original magnification, ×400. Values are presented as mean + SEM. *$P < 0.05$.

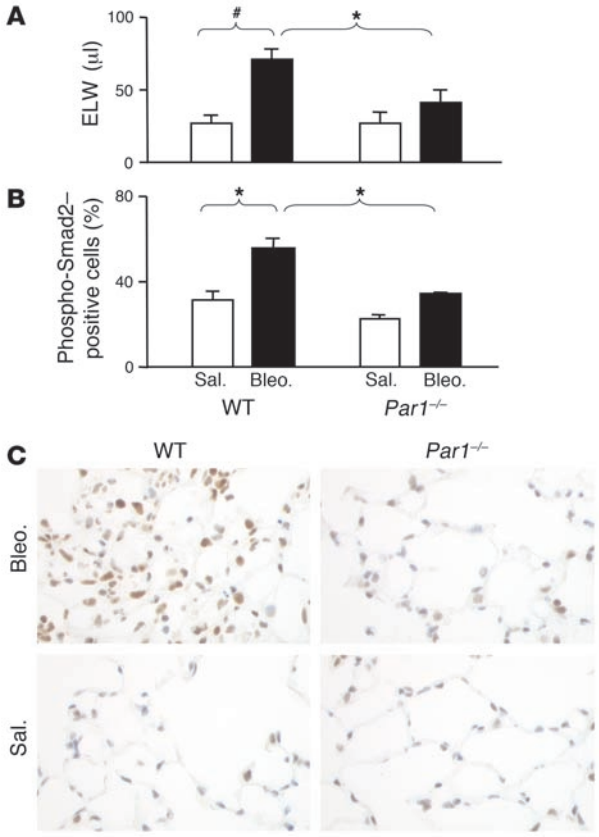

Figure 8

Par1$^{-/-}$ mice instilled with intratracheal bleomycin have reduced permeability and TGF-β activation compared with WT control. (**A**) WT or *Par1*$^{-/-}$ mice were instilled with saline (Sal.; white bars) or 0.05 U bleomycin (Bleo.; black bars). ELW was measured as described. Bleomycin, $n = 6$; and saline, $n = 5$. (**B**) Quantification of nuclear localized phospho-Smad2 immunostaining in WT or *Par1*$^{-/-}$ mice instilled with saline (white bars) or 0.05 U bleomycin (black bars). WT mice, $n = 4$; *Par1*$^{-/-}$, bleomycin, $n = 4$; and *Par1*$^{-/-}$, saline, $n = 3$. (**C**) Representative histological sections showing nuclear localized phospho-Smad2 immunostaining in the lung of WT or *Par1*$^{-/-}$ mice. Original magnification, ×400. Values are presented as mean + SEM. $^{\#}P < 0.005$, $^{*}P < 0.05$.

mechanisms that regulate $\alpha_v\beta_6$-mediated TGF-β activation were completely unknown. The data presented here demonstrate that $\alpha_v\beta_6$-mediated TGF-β activation can be induced by agonists of PAR1. We have shown that the signal from the PAR1 receptor to $\alpha_v\beta_6$ does not require synthesis of new protein but is rather mediated via direct "inside-out" signaling. We have also shown that the PAR1 receptor signals to the $\alpha_v\beta_6$ integrin via RhoA and Rho kinase. Because of the well-known effects of RhoA in reorganizing actin, these findings are consistent with our earlier observation that $\alpha_v\beta_6$-mediated TGF-β activity is completely inhibited by an inhibitor of actin polymerization, cytochalasin D (1). Finally, we show that PAR1 activation in the setting of high-tidal-volume ventilation causes an $\alpha_v\beta_6$-dependent increase in lung edema, whereas in *Par1*$^{-/-}$ mice there is reduced permeability, and TGF-β activity, following bleomycin-induced lung injury. These studies demonstrate a novel mechanism by which PAR1 stimulation can lead to acute lung injury.

Although many mechanisms have been shown to activate TGF-β, it appears that in cells where $\alpha_v\beta_6$ is present it is the predominant mechanism by which TGF-β is activated under basal conditions. In all the cell types we tested there was complete blockade of TGF-β activity using an $\alpha_v\beta_6$ blocking antibody, as assessed by comparison with a pan–TGF-β blocking antibody. There are a number of possible explanations for how the pathway we describe here could induce $\alpha_v\beta_6$-mediated TGF-β activation. One possibility is that PAR1 stimulation could increase the affinity of $\alpha_v\beta_6$ for LAP, in a manner analogous to the effects of a similar pathway on the platelet integrin $\alpha_{IIb}\beta_3$. However, we do not favor this possibility. In contrast to the platelet integrin, which cannot mediate adhesion to ligands in the absence of external signals, $\alpha_v\beta_6$ is constitutively capable of supporting adhesion to LAP in all of the cell lines we have expressed it in. Another intriguing possibility is that a change in cell shape induced by Rho kinase activation exerts a mechanical force on the latent complex, inducing a conformational change that allows active TGF-β to productively contact its receptors on adjacent cells. Recent evidence in support of this hypothesis comes from work demonstrating the critical role of latent TGF-β–binding protein-1 (LTBP-1), another component of latent TGF-β, in $\alpha_v\beta_6$-mediated TGF-β activation (22). That study demonstrated that LTBP-1 was absolutely essential to this process and that the requirement for LTBP-1 could be satisfied by a short fusion protein containing only the regions of LTBP-1 required for disulfide linkage to LAP and for cross-linking of LTBP-1 to the ECM. These findings support a critical role for LTBP-1 as a mechanical tether for latent complexes of TGF-β. There is precedent for integrins modulating the behavior of extracellular proteins through mechanical changes in conformation. Previous work has shown that the $\alpha_v\beta_1$ integrin contributes to fibronectin matrix assembly by inducing a conformational change in fibronectin that reveals a cryptic site required for formation of fibronectin polymers (23). Importantly, those effects were also shown to be mediated by RhoA.

It is likely that other agonists could also induce $\alpha_v\beta_6$-dependent TGF-β activation, but none has yet been described. Our data demonstrate that *Par1*$^{-/-}$ fibroblasts, although unable to respond to PAR1 agonists, have a background level of $\alpha_v\beta_6$-dependent TGF-β activation similar to that seen in WT fibroblasts and *Par1*$^{-/-}$ fibroblasts reconstituted with PAR1. Although the cause of this background $\alpha_v\beta_6$-dependent TGF-β activity is unclear, it is of note that it is much greater in fibroblasts than in IMLE cells, and not observed in polarized cultures of normal bronchial epithelial cells. It is possible that other activators of Rho kinase may be contributing to this observed baseline TGF-β activation, since the inhibitor of Rho kinase reduced baseline TGF-β activity.

PAR1 is a G protein–coupled receptor that couples to the heterotrimeric G proteins Gαi, Gαq, and Gα12/13. The G proteins Gα12 and Gα13 are known to be critical in thrombin-induced RhoA activation in platelets (24) and have been shown to activate RhoA downstream of other receptors, such as lysophosphatidic acid receptors (25). Recently, Gα13 has been shown to be the critical effector of agonist-induced platelet shape change and, by extension, RhoA activation in platelets (26). In astrocytes Gα12 has been shown to be crucial in thrombin-mediated Rho-dependent cytoskeletal changes (27). To what extent these differences are cell type specific or reflect redundancy remains uncertain. Based on these results in other cells, we speculate that PAR1 signals via either Gα12 or Gα13 to induce $\alpha_v\beta_6$-mediated TGF-β activation.

Our data demonstrate that PAR1 can cause increased lung edema when the lungs are ventilated at high tidal volumes, and that this effect is mediated by the $\alpha_v\beta_6$ integrin. However, when the lungs are not mechanically ventilated, PAR1 stimulation has little effect (data not shown). This suggests that in the absence of mechanical ventilation, any increase in TGF-β activity induced by PAR1 is not sufficient to cause pulmonary edema. It is possible that in vivo in the normal lung, PAR1 is only able to mediate enough intracellular "pull" to activate TGF-β in combination with the extracellular stretch caused by large-tidal-volume ventilation. We have previously shown that activation of TGF-β by $\alpha_v\beta_6$ requires binding of the integrin to the LAP of the small latent complex and direct cell-cell contact between cells expressing the integrin and cells expressing the TGF-β receptor (1), which implies very tight spatial control of this system. It is also possible that ventilation may lead to redistribution of $\alpha_v\beta_6$ or the TGF-β receptor, thus permitting PAR1-induced $\alpha_v\beta_6$-mediated TGF-β activation to occur.

We also show that PAR1 plays a physiological role in the induction of acute lung injury. Like mice lacking the $\alpha_v\beta_6$ integrin, mice lacking PAR1 are significantly protected from the increase in lung edema induced by intratracheal instillation of bleomycin. In murine models, activation of TGF-β by $\alpha_v\beta_6$ is important in the pathogenesis of acute lung injury and pulmonary and renal fibrosis, but until now the mechanisms by which this process is regulated have been poorly understood. Here we show, for the first time to our knowledge, that a receptor for thrombin, a molecule that is important in the pathogenesis of acute lung injury, induces $\alpha_v\beta_6$-mediated TGF-β activation in epithelial cells. Furthermore, we demonstrate that the signal is a direct "inside-out" signal mediated via the small GTPase RhoA and its downstream effector Rho kinase. Finally, we show that during mechanical ventilation, PAR1 stimulation is able to exacerbate lung injury by increasing lung permeability, whereas the absence of PAR1 protects against acute lung injury and reduces TGF-β activation. These data illustrate a novel mechanism in the pathogenesis of both ventilator-associated and acute lung injury. These results suggest that targeting the $\alpha_v\beta_6$ integrin, PAR1, or its downstream effectors RhoA and Rho kinase could be an effective intervention in acute lung injury or other disorders in which $\alpha_v\beta_6$-mediated TGF-β activation plays an important role.

Methods

Cell lines, antibodies, and reagents. The *Par1*$^{-/-}$ fibroblasts were a gift of Shaun Coughlin (University of California, San Francisco, San Francisco, California, USA) (17). Adenoviruses encoding either constitutively active (RhoA G-V14) or dominant-negative (RhoA T-N19) forms of RhoA that also express enhanced GFP were generated as previously described (28). The proximal large airway epithelial (normal human bronchial epithelial) cells were obtained commercially from Cambrex, and the TML epithelial reporter cells stably expressing firefly luciferase under the control of a TGF-β–sensitive portion of the plasminogen activator inhibitor-1 promoter were a gift from Dan Rifkin (New York University, New York, New York, USA). The $\alpha_v\beta_6$ blocking antibody 3G9 (29) was provided by Paul Weinreb and Shelia Violette (Biogen Idec). All other reagents were commercially obtained. The antibodies used were mouse monoclonal anti–TGF-β (clone 1D11; R&D Systems), rat polyclonal anti–β_4 integrin subunit (BD), mouse monoclonal anti-pancytokeratin (Sigma-Aldrich), mouse monoclonal anti-PAR1 (BD), and rabbit polyclonal anti–phospho-Smad2 and anti–total Smad2 (Cell Signaling Technology). The stimulants used were thrombin (Amersham Biosciences); the PAR1 agonist peptides SFLLRN, FSLLRN, TFLLRN, and FTLLRN (Anaspec); and TGF-β1 (R&D Systems). Inhibitors used were the Rho kinase inhibitor Y-27632 and cycloheximide (Calbiochem).

Generation of IMLE cells. The Immortomouse (Charles River Laboratories) is transgenic for a ubiquitously expressed temperature-sensitive SV40 large T antigen to permit propagation of immortalized cells at permissive temperatures (33°C) and reversion to their primary phenotype at nonpermissive temperatures (39°C). The Immortomouse was bred with the *Itgb6*$^{-/-}$ mouse, and isolation of mouse lung epithelial cells was performed. Briefly, adult *Itgb6*$^{-/-}$ Immortomice were sacrificed (50 mg/ml Nembutal and 1,000 U/ml heparin) and their lungs perfused with Krebs (–) buffer (133 mM NaCl, 5.2 mM KCl, 2.59 mM Na_2PO_4, 10.3 mM HEPES, 0.2 mM EGTA, 5 mM glucose). The lungs were removed en bloc and lavaged 8 times with Krebs (–) followed by 2 times with Krebs (+) buffer (133 mM NaCl, 5.2 mM KCl, 2.59 mM Na_2PO_4, 10.3 mM HEPES, 5 mM glucose, 1.89 mM $CaCl_2$, 1.29 mM $MgSO_4$). The lungs were digested by intratracheal instillation of 40 ml of 4.3 U/ml elastase in Krebs (+) buffer for 30 minutes at 37°C. The airways were dissected and the lungs minced in 2 mg DNase I (Sigma-Aldrich) before elastase inactivation with 10% FCS in DMEM. The minced lungs were sequentially filtered before cell culture propagation at the permissive temperature of 33°C. To remove any contaminating fibroblasts, cells underwent positive selection using an anti–β_4 integrin antibody by fluorescence-activated cell sorting as described below.

Generation of stable cell lines. IMLE cells and mouse fibroblasts were infected with WT human β_6 subunit in the retroviral vector pWZL. Retroviruses were generated by Lipofectamine-mediated (Invitrogen) transfection of the thi-ε replication-incompetent ectropic virus packaging cell line. The virus-containing supernatant was harvested and filtered through a 0.22-μM filter and then added to 50% confluent cultures in the presence of 5 μg/ml Polybrene and cultured for 24 hours. The virus-containing medium was removed, and cells were cultured in 5% DMEM-FCS containing 5 μg/ml blasticidin (Sigma-Aldrich). Cells expressing the $\alpha_v\beta_6$ integrin were identified by flow cytometry with the anti-$\alpha_v\beta_6$ antibody 3G9. Fluorescence-activated cell sorting was performed to isolate populations of cells with high levels of $\alpha_v\beta_6$ on their surface. All cell lines continuously expressed high surface levels of $\alpha_v\beta_6$ as determined by flow cytometry with 3G9.

Adenoviral infection. Adenoviruses were amplified by infection of AD293 cells (Invitrogen) with crude viral lysate. AD293 cells were observed under inverse fluorescence microscopy. When all cells were expressing GFP and showing cytopathic effects, they were harvested with normal growth media as crude viral lysate. The lysate underwent a single freeze-thaw cycle before 40-μm filtration. Fibroblasts were cultured as described and, before reaching confluence, were harvested by trypsinization. The fibroblasts were then resuspended with adenovirus-containing media (10:1 ratio of normal growth medium to crude viral lysate) for 2 hours. The medium was replaced with normal growth medium, and cells were replated on tissue culture–treated 10-cm dishes for 16 hours before cell sorting.

Flow cytometry. Cultured cells were harvested by trypsinization. Nonspecific binding was blocked with normal goat serum at 4°C for 20 minutes. Cells were then incubated with primary antibody for 20 minutes at 4°C, followed by secondary goat anti-mouse antibody conjugated with PE (Chemicon International). Between incubations, cells were washed twice with PBS. Stained cells were resuspended in 100 μl of PBS, and the fluorescence was quantified on 10,000 cells with a FACScan flow cytometer (BD).

Calcium mobilization assay. Cultured cells were harvested by enzyme-free cell dissociation buffer (Invitrogen), and pelleted by centrifugation. Cells were resuspended at 2×10^6 per milliliter in RPMI containing 25 mM HEPES and 1 mg/ml BSA supplemented with 5% cell dissociation buffer, and loaded with the calcium indicator fluo-4AM (Invitrogen) at a final concentration of 10 μM for 30 minutes at room temperature. Cells were washed twice by centrifugation and resuspended in indicator-free RPMI

for a further 30 minutes to allow complete de-esterification of intracellular acetoxymethyl esters. Fluorescence measurements, reflecting elevations of intracellular calcium, were conducted at 24°C using a GENios Pro microplate reader (Tecan), with an excitation wavelength of 480 nm and emission recorded at 530 nm. Fluorescence signals caused by test agonists were compared with fluorescence peak heights of replicate cell suspensions treated with 10 μM of ionophore A23187 (Sigma-Aldrich)

TML cell assay. Experimental cell lines were plated at 2.5×10^4 cells per milliliter in 10% DMEM-FCS for 4 hours to allow adhesion and cell spreading. This medium was then changed to serum-free DMEM overnight. Immediately after sorting, cells infected with GFP-tagged constructs were plated at 4×10^4 in serum-free media for 4 hours before stimulation and TGF-β activity assessments. TML cells were harvested by trypsinization and resuspended in serum-free DMEM at 5×10^5 cells per milliliter. An aliquot of TML cells was removed and mixed with $\alpha_v\beta_6$ or TGF-β antibody. The medium was then removed from the experimental cells, and an equal volume (100 μl) of TML cells (with or without antibodies) and medium containing experimental stimulant or inhibitor was added. The coculture proceeded overnight, and cells were washed once in PBS before cell lysis for 20 minutes at 4°C in reporter lysis buffer (Promega). The cell layer was agitated with a pipette and centrifuged at 1500 *g* for 5 minutes at 4°C. The supernatant was added to luciferin assay buffer (Promega) and the luminescence measured at 24°C in a GENios Pro microplate reader (Tecan).

Western blot analysis. Cells were lysed on ice for 20 minutes in buffer containing 50 mM Tris, 150 mM NaCl, 20 mM NaF, 1 mM $NaVaO_3$, 1 mM EDTA, 1 μM PMSF glycerol, 1% vol/vol Triton X-100, 0.1% vol/vol sodium dodecyl sulfate, and a protease inhibitor cocktail (Sigma-Aldrich). Total protein was measured using a bicinchoninic acid assay (Pierce Biotechnology). Approximately 100 μg of protein was fractionated by SDS-PAGE, transferred onto PVDF membranes (Hybond-ECL; Amersham Biosciences), and incubated with blocking buffer containing 5% nonfat dry milk in Tris-buffered saline with Tween (TBST) (50 mM Tris, 150 mM NaCl, 0.1% Tween-20, pH 7.4) for 1 hour. For examination of Smad2 phosphorylation, membranes were incubated with a phospho-Smad2 polyclonal rabbit anti-mouse antibody (Cell Signaling Technology) in 5% skimmed milk TBST overnight at 4°C. All blots were then washed with TBST and incubated for 1 hour at room temperature with HRP-conjugated anti-rabbit IgG. After further washing in TBST, immunoreactive bands were visualized by ECL (Amersham Biosciences) according to the manufacturer's instructions. For examination of total Smad2 levels, the blots were stripped using Restore stripping buffer (Pierce Biotechnology) for 30 minutes at room temperature before immunoblotting using a total-Smad2 polyclonal rabbit anti-mouse antibody (Cell Signaling Technology) and the protocol described above.

Immunocytochemistry. Immortomouse cells were grown on coverslips coated with 10 μg/ml collagen (Sigma-Aldrich). Cells were fixed in 4% paraformaldehyde and permeabilized for 5 minutes in 0.5% Triton X-100. The cell layer was washed twice with PBS before blocking of nonspecific binding with Mouse-on-Mouse blocking reagent (Vector Laboratories) or normal goat serum for 1 hour at room temperature. After washing twice in PBS, FITC-labeled primary antibody (Sigma-Aldrich) was added at a 1:20 dilution for 2 hours at room temperature. The cell layer was then incubated with 1:10,000 DAPI for 10 minutes and washed twice with PBS before air-drying and mounting. Immunofluorescence was visualized by microscopy (Leica DM5000B; Leica Microsystems).

Ventilator-induced pulmonary edema model. *Itgb6*$^{-/-}$ and WT control mice were bred at UCSF, and C57BL/6J mice (8 weeks old) were purchased from Jackson Laboratory. All experiments were approved by the UCSF Institutional Animal Care and Use Committee. Mice were injected i.p. with either anti-$\alpha_v\beta_6$ mAb 3G9 (1 mg/kg; Biogen Idec) or control antibody (1E6) 16 hours before the experiment. Mice were anesthetized with i.p. ketamine (90 mg/kg) and xylazine (10 mg/kg), and HBSS (25 ml), TFLLRN (25 mM, 25 ml), or FTLLRN (25 mM, 25 ml) was instilled into the trachea. Twenty-five minutes later, the trachea was cannulated with a PE-90 cannula, and mice were ventilated using a previously validated protocol with minor modifications (30). Briefly, mice were ventilated with room air at a tidal volume of 24 ml/kg, at a frequency of 40 strokes per minute, by a rodent respirator (Harvard Apparatus). Mice were given an i.p. injection of 0.9% saline (0.01 ml/g/h) to maintain stable hemodynamics. Body temperature was maintained at 37°C with a heating pad and monitored by a rectal thermometer (Fisher Scientific). The right jugular vein was catheterized for administration of radioactive label (0.05 μCi ^{125}I-albumin; Iostex Diagnostics Inc.) to evaluate lung vascular permeability.

Bleomycin model of acute lung injury. WT and *Par1*$^{-/-}$ mice were bred at University College London. All animal studies were approved by the University College London Biological Services Ethical Review Committee and licensed under the Animals (Scientific Procedures) Act 1986, Home Office, London, United Kingdom. Mice (8 weeks old) were anesthetized with inhaled halothane (3%) in a stream of oxygen (2 l/min). Mice received a single intratracheal instillation of bleomycin (0.05 IU in 50 μl sterile saline; Kyowa-Hakko) or saline alone. We have previously shown that $\alpha_v\beta_6$ integrin–mediated lung permeability changes are maximal at 5 days (9); therefore animals were terminally anesthetized, using an i.p. injection of 100 μl of pentobarbitone sodium (200 mg/ml; sanofi aventis), at this time point. Lungs and blood were removed for permeability measurements as described below. For analysis of TGF-β, the pulmonary vasculature was perfused with PBS and the lungs were inflated by intratracheal instillation of 4% paraformaldehyde at 20 cm H_2O. The heart and lungs were removed en bloc, immersed in 4% paraformaldehyde overnight at 4°C, and processed to paraffin wax.

Measurement of ELW and lung extravascular plasma equivalents. The mice were sacrificed after 2 hours of high-tidal-volume ventilation. The lungs were removed, counted in a gamma counter (Packard; PerkinElmer), weighed, and homogenized after addition of 1 ml of distilled water. Blood was collected through right ventricular puncture. The lung homogenate was weighed and an aliquot centrifuged (16,000 *g*, 8 minutes) for assay of hemoglobin concentration in the supernatant. A second aliquot of homogenate, supernatant, and blood was weighed and then desiccated in an oven (60°C for 24 hours) for gravimetric determination of ELW. The lung wet-to-dry weight ratio (lung W/D ratio) was calculated by a standard formula (9). ELW was calculated using the following formula: (lung W/D ratio$_{experimental}$ × lung dry weight$_{experimental}$) – (lung W/D ratio$_{normal}$ × lung dry weight$_{experimental}$) × 1,000. Lung extravascular plasma equivalents (EVPE; index of lung vascular permeability) were calculated as the counts of ^{125}I-albumin in the lung tissue divided by the counts of ^{125}I-albumin in the plasma (9).

Measurement of in vivo TGF-β activity. Five-micrometer-thick lung tissue sections were cut, dewaxed in xylene, rehydrated through decreasing concentrations of ethanol, and washed in Tris-buffered saline. Antigens were unmasked by microwaving of sections in 10 mmol/l citrate buffer, pH 6.0 (twice for 10 minutes), and immunostaining was undertaken using the avidin-biotinylated enzyme complex method (Vector Laboratories) with antibodies against phospho-Smad2 at a concentration of 50 ng/ml, and equivalent concentrations of polyclonal nonimmune IgG controls. After incubation with biotin-conjugated secondary antibody and subsequently with streptavidin solution, color development was performed using 3,3′-diaminobenzidine tetrahydrochloride (Vector Laboratories). Sections were counterstained using Gill-2 hematoxylin (Thermo Electron Corp.). In order to quantify TGF-β activity, cells with nuclear localized immunostain were counted. Three random sections of lung parenchyma were assessed at high power for each of the 5 lobes of each mouse.

Statistics. Statistical comparisons were performed with an unpaired 2-tailed Student's *t* test. *P* values less than 0.05 were considered statistically significant.

Acknowledgments

This work was funded by grants from the Arthritis Research Campaign (to R.G. Jenkins) and the Wellcome Trust (to R.C. Chambers and G.J. Laurent) and by grants HL56385, HL64353, HL53949, and HL66600 (to D. Sheppard) and HL51854, HL51856, and HL74005 (to M.A. Matthay) from the National Heart, Lung, and Blood Institute. We would like to thank Steve Bottoms for help in preparing and blinding the histological specimens.

Received for publication October 20, 2005, and accepted in revised form April 11, 2006.

Address correspondence to: Dean Sheppard, Lung Biology Center, University of California, San Francisco, 1550 4th Street, San Francisco, California 94158, USA. Phone: (415) 514-4175; Fax: (415) 514-4278; E-mail: dean.sheppard@ucsf.edu.

1. Munger, J.S., et al. 1999. The integrin alpha v beta 6 binds and activates latent TGF beta 1: a mechanism for regulating pulmonary inflammation and fibrosis. *Cell*. **96**:319–328.
2. Mu, D., et al. 2002. The integrin alpha(v)beta8 mediates epithelial homeostasis through MT1-MMP-dependent activation of TGF-beta1. *J. Cell Biol*. **157**:493–507.
3. Lawrence, D.A., Pircher, R., and Jullien, P. 1985. Conversion of a high molecular weight latent beta-TGF from chicken embryo fibroblasts into a low molecular weight active beta-TGF under acidic conditions. *Biochem. Biophys. Res. Commun*. **133**:1026–1034.
4. Pircher, R., Jullien, P., and Lawrence, D.A. 1986. Beta-transforming growth factor is stored in human blood platelets as a latent high molecular weight complex. *Biochem. Biophys. Res. Commun*. **136**:30–37.
5. Lyons, R.M., Gentry, L.E., Purchio, A.F., and Moses, H.L. 1990. Mechanism of activation of latent recombinant transforming growth factor beta 1 by plasmin. *J. Cell Biol*. **110**:1361–1367.
6. Schultz-Cherry, S., and Murphy-Ullrich, J.E. 1993. Thrombospondin causes activation of latent transforming growth factor-beta secreted by endothelial cells by a novel mechanism. *J. Cell Biol*. **122**:923–932.
7. Yu, Q., and Stamenkovic, I. 2000. Cell surface-localized matrix metalloproteinase-9 proteolytically activates TGF-beta and promotes tumor invasion and angiogenesis. *Genes Dev*. **14**:163–176.
8. Morris, D.G., et al. 2003. Loss of integrin alpha(v)beta6-mediated TGF-beta activation causes Mmp12-dependent emphysema. *Nature*. **422**:169–173.
9. Pittet, J.F., et al. 2001. TGF-β is a critical mediator of acute lung injury. *J. Clin. Invest*. **107**:1537–1544.
10. Ma, L.J., et al. 2003. Transforming growth factor-beta-dependent and -independent pathways of induction of tubulointerstitial fibrosis in beta6(–/–) mice. *Am. J. Pathol*. **163**:1261–1273.
11. Huang, X., Wu, J., Zhu, W., Pytela, R., and Sheppard, D. 1998. Expression of the human integrin beta6 subunit in alveolar type II cells and bronchiolar epithelial cells reverses lung inflammation in beta6 knockout mice. *Am. J. Respir. Cell Mol. Biol*. **19**:636–642.
12. Hakkinen, L., et al. 2004. Increased expression of beta6-integrin in skin leads to spontaneous development of chronic wounds. *Am. J. Pathol*. **164**:229–242.
13. Munger, J.S., Harpel, J.G., Giancotti, F.G., and Rifkin, D.B. 1998. Interactions between growth factors and integrins: latent forms of transforming growth factor-beta are ligands for the integrin alphavbeta1. *Mol. Biol. Cell*. **9**:2627–2638.
14. Schnapp, L.M., Breuss, J.M., Ramos, D.M., Sheppard, D., and Pytela, R. 1995. Sequence and tissue distribution of the human integrin alpha 8 subunit: a beta 1-associated alpha subunit expressed in smooth muscle cells. *J. Cell Sci*. **108**:537–544.
15. Fuchs-Buder, T., et al. 1996. Time course of procoagulant activity and D dimer in bronchoalveolar fluid of patients at risk for or with acute respiratory distress syndrome. *Am. J. Respir. Crit. Care Med*. **153**:163–167.
16. Kipnis, E., et al. 2004. Massive alveolar thrombin activation in Pseudomonas aeruginosa-induced acute lung injury. *Shock*. **21**:444–451.
17. Trejo, J., Connolly, A.J., and Coughlin, S.R. 1996. The cloned thrombin receptor is necessary and sufficient for activation of mitogen-activated protein kinase and mitogenesis in mouse lung fibroblasts. Loss of responses in fibroblasts from receptor knockout mice. *J. Biol. Chem*. **271**:21536–21541.
18. Camerer, E., Kataoka, H., Kahn, M., Lease, K., and Coughlin, S.R. 2002. Genetic evidence that protease-activated receptors mediate factor Xa signaling in endothelial cells. *J. Biol. Chem*. **277**:16081–16087.
19. Howell, D.C., et al. 2001. Direct thrombin inhibition reduces lung collagen, accumulation, and connective tissue growth factor mRNA levels in bleomycin-induced pulmonary fibrosis. *Am. J. Pathol*. **159**:1383–1395.
20. Lerner, D.J., Chen, M., Tram, T., and Coughlin, S.R. 1996. Agonist recognition by proteinase-activated receptor 2 and thrombin receptor. Importance of extracellular loop interactions for receptor function. *J. Biol. Chem*. **271**:13943–13947.
21. Blackhart, B.D., et al. 1996. Ligand cross-reactivity within the protease-activated receptor family. *J. Biol. Chem*. **271**:16466–16471.
22. Annes, J.P., Chen, Y., Munger, J.S., and Rifkin, D.B. 2004. Integrin alphaVbeta6-mediated activation of latent TGF-beta requires the latent TGF-beta binding protein-1. *J. Cell Biol*. **165**:723–734.
23. Zhong, C., et al. 1998. Rho-mediated contractility exposes a cryptic site in fibronectin and induces fibronectin matrix assembly. *J. Cell Biol*. **141**:539–551.
24. Klages, B., Brandt, U., Simon, M.I., Schultz, G., and Offermanns, S. 1999. Activation of G12/G13 results in shape change and Rho/Rho-kinase-mediated myosin light chain phosphorylation in mouse platelets. *J. Cell Biol*. **144**:745–754.
25. Wang, Q., et al. 2004. Thrombin and lysophosphatidic acid receptors utilize distinct rhoGEFs in prostate cancer cells. *J. Biol. Chem*. **279**:28831–28834.
26. Moers, A., et al. 2003. G_{13} is an essential mediator of platelet activation in hemostasis and thrombosis. *Nat. Med*. **9**:1418–1422.
27. Majumdar, M., Seasholtz, T.M., Buckmaster, C., Toksoz, D., and Brown, J.H. 1999. A rho exchange factor mediates thrombin and Galpha(12)-induced cytoskeletal responses. *J. Biol. Chem*. **274**:26815–26821.
28. Bayless, K.J., and Davis, G.E. 2004. Microtubule depolymerization rapidly collapses capillary tube networks in vitro and angiogenic vessels in vivo through the small GTPase Rho. *J. Biol. Chem*. **279**:11686–11695.
29. Weinreb, P.H., et al. 2004. Function-blocking integrin alphavbeta6 monoclonal antibodies: distinct ligand-mimetic and nonligand-mimetic classes. *J. Biol. Chem*. **279**:17875–17887.
30. Chavolla-Calderon, M., Bayer, M.K., and Fontan, J.J. 2003. Bone marrow transplantation reveals an essential synergy between neuronal and hemopoietic cell neurokinin production in pulmonary inflammation. *J. Clin. Invest*. **111**:973–980. doi:10.1172/JCI200317458.